NASA TN D-1427

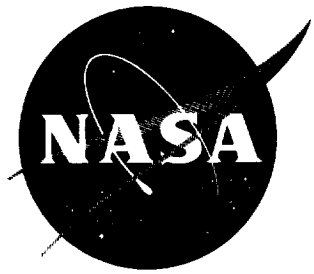

TECHNICAL NOTE

D-1427

ATMOSPHERE ENTRIES WITH SPACECRAFT LIFT-DRAG RATIOS MODULATED TO LIMIT DECELERATIONS

By Lionel L. Levy, Jr.

Ames Research Center
Moffett Field, Calif.

NATIONAL AERONAUTICS AND SPACE ADMINISTRATION

WASHINGTON

October 1962

NATIONAL AERONAUTICS AND SPACE ADMINISTRATION

TECHNICAL NOTE D-1427

ATMOSPHERE ENTRIES WITH SPACECRAFT LIFT-DRAG RATIOS MODULATED TO LIMIT DECELERATIONS

By Lionel L. Levy, Jr.

SUMMARY

An analysis has been made of atmosphere entries for which the spacecraft lift-drag ratios were modulated to limit the maximum deceleration. The parts of the drag polars used during modulation were from maximum lift coefficient to minimum drag coefficient. Five drag polars of different shapes were assumed for the spacecraft. The entries covered wide ranges of initial velocity, initial flight-path angle, initial m/C_DA, and maximum lift-drag ratio. Two-dimensional trajectory calculations were made for a nonrotating, spherical earth with an exponential atmosphere. The results of the analysis indicate for four of the five drag polars that, relative to the maximum deceleration of an unmodulated entry at maximum lift-drag ratio, the greatest reduction in maximum deceleration obtainable by modulation depends upon a single parameter. This parameter is the ratio of the value of the aerodynamic resultant-force coefficient at minimum drag coefficient to the value at maximum lift coefficient. Thus, the reduction in maximum deceleration is independent of initial velocity, initial flight-path angle, initial m/C_DA, maximum lift-drag ratio, and the shape of the drag polar. For the fifth drag polar, the reduction in maximum deceleration was found to depend upon the maximum lift-drag ratio. Also, relative to the depth of a given deceleration-limited corridor, the greatest increase in corridor depth obtainable by modulation (for four of the five drag polars) depends upon the same ratio of aerodynamic resultant-force coefficients. The fractional increase in corridor depth can be expressed as an empirically determined analytical function of this ratio.

INTRODUCTION

The magnitude of the reduction in maximum deceleration obtainable by continuously varying (modulating) the aerodynamic coefficients of lifting spacecraft during atmosphere entry has been studied in references 1 through 5. In these studies the results generally were obtained for a spacecraft with a particular type of drag polar and for several values of maximum lift-drag ratio and initial velocity.

The purpose of the present investigation is to determine the effects of type of drag polar, initial velocity, initial flight-path angle,

initial m/C_DA, and maximum lift-drag ratio on the reduction in maximum deceleration obtainable by continuous modulation. To accomplish this purpose a trajectory analysis was made on an IBM 7090 computing machine to solve the two-dimensional equations of motion of reference 6 for entries into an exponential atmosphere of a spherical nonrotating earth. Most of the results were obtained for entries at escape velocity of spacecraft with maximum lift-drag ratios of 0.5. For these spacecraft, the convective and radiative heating and range were also determined for entries at escape velocity.

NOTATION

A	reference area for drag and lift, ft^2
C_D	drag coefficient, $\frac{2D}{\rho V^2 A}$
$C_{D_{min}}$	minimum drag coefficient
C_L	lift coefficient, $\frac{2L}{\rho V^2 A}$
C_R	aerodynamic resultant-force coefficient, $C_D\sqrt{1 + (L/D)^2}$
D	drag force, lb
g	local gravitational acceleration, ft sec^{-2}
G	deceleration in g units
L	lift force, lb
m	mass of spacecraft, slugs
q	total heat absorbed at the stagnation point, Btu ft^{-2}
$\dot{q}$	heating rate at the stagnation point, $\frac{dq}{dt}$, Btu $ft^{-2}sec^{-1}$
r	distance from the center of planet, ft
r_o	radius of planet, 2.0926×10^7 ft for earth
R	radius of curvature of spacecraft surface at the stagnation point (unswept for winged spacecraft), ft
s	range, ft

t	time, sec
u	tangential velocity component normal to a radius vector, ft sec^{-1}
v	radial velocity component, ft sec^{-1}
V	resultant velocity, ft sec^{-1}
$\overline{V}$	dimensionless velocity ratio, $\frac{V}{\sqrt{\mu/r}}$
y	altitude, ft
α	angle of attack of spacecraft, deg
β	atmosphere density decay parameter, 1/23,500 ft^{-1} for earth
γ	flight-path angle relative to the local horizontal, negative for descent, deg
μ	gravitational constant, 1.4078×10^{16} $ft^3 sec^{-2}$ for earth
ρ	atmosphere density, slug ft^{-3}
ρ_o	atmosphere density at planet surface, 0.00238 slug ft^{-3} for earth
$\bar{\rho}_o$	mean value for exponential approximation to atmosphere density-altitude relation, 0.0027 slug ft^{-3} for earth

Subscripts

c	convective
i	initial
max	maximum
mod	modulated entry
ov	overshoot boundary
p	vacuum perigee
un	undershoot boundary
unmod	unmodulated entry
r	radiative

ANALYSIS

A trajectory analysis has been made utilizing the solution of two-dimensional equations of motion for entries into an exponential atmosphere of a nonrotating spherical earth. The polar coordinate system with velocity components, aerodynamic forces, and flight-path angle is defined in sketch (a). The differential equations for the velocity in the radial and tangential directions are, respectively, (see ref. 6)

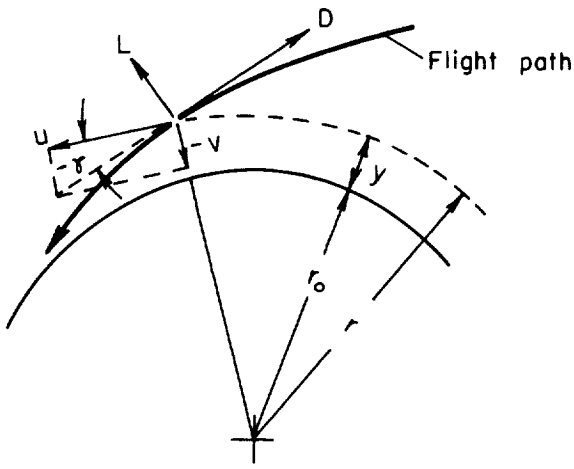

Sketch (a)

$$\frac{dv}{dt} = -g + \frac{u^2}{r} + \frac{L}{m}\cos\gamma - \frac{D}{m}\sin\gamma \tag{1}$$

$$\frac{du}{dt} = -\frac{uv}{r} - \frac{D}{m}\cos\gamma - \frac{L}{m}\sin\gamma \tag{2}$$

where

$$\tan\gamma = \frac{v}{u} \tag{3}$$

$$r = r_o + y \tag{4}$$

and g is the local gravitational acceleration given by

$$g = \frac{\mu}{r^2} \tag{5}$$

The constant μ in equation (5) is the gravitational constant defined by Newton's inverse square law of gravitational attraction. The differential equations employed for the altitude and range are, respectively,

$$\frac{dy}{dt} = v \tag{6}$$

$$\frac{ds}{dt} = u \tag{7}$$

The differential equations used for the total laminar convective heat (after ref. 6) and the radiative heat (ref. 7) absorbed per unit area at the stagnation point are, respectively,

$$\frac{dq_c}{dt} = \dot{q}_c = \frac{16{,}600}{\sqrt{R}} \sqrt{\frac{\rho}{\rho_o}} \left(\frac{V}{\sqrt{gr}}\right)^3 \tag{8}$$

$$\frac{dq_r}{dt} = \dot{q}_r = R10^{f(y,V)} \tag{9}$$

where R is the radius of curvature of the spacecraft surface at the stagnation point (an unswept stagnation point for winged spacecraft), ρ is the local atmosphere density given by

$$\rho = \bar{\rho}_o e^{-\beta y} \tag{10}$$

and V is the resultant velocity given by

$$V = \sqrt{u^2 + v^2} \tag{11}$$

The radiative heating rate per unit area at the stagnation point is obtained from an interpolation of a table for the logarithm of equation (9); that is,

$$\log_{10}\left(\frac{\dot{q}_r}{R}\right) = f(y,V) \tag{12}$$

Values of $(\dot{q}_r/R)$ as a function of altitude and velocity for air in equilibrium were obtained from reference 7.

The six equations (1), (2), (6), (7), (8), and (9) were programmed for simultaneous solution on an IBM 7090 computing machine for entries during which the spacecraft aerodynamic coefficients were constant and for entries during which these coefficients were varied (modulated) to reduce the maximum deceleration as much as possible. In the analysis the resultant deceleration G is given by

$$G = \frac{1}{g(m/A)} \left(\frac{1}{2} \rho V^2\right) C_R \tag{13}$$

where C_R, the aerodynamic resultant-force coefficient, is

$$C_R = C_D \sqrt{1 + (L/D)^2} \tag{14}$$

For entries modulated to reduce the maximum deceleration, the deceleration is constant during the modulation period.

Corridor Depth

In general, corridor depth is defined as the difference in perigee altitudes of two vacuum trajectories each of which is identified by the associated flight-path angle at a given initial altitude and velocity. The flight-path angle associated with the higher of the two perigee altitudes is usually referred to as the angle for an overshoot boundary, and the angle associated with the lower of the two perigee altitudes is referred to as the angle for an undershoot boundary (see, e.g., ref. 3). The relationship between perigee altitude, flight-path angle, and velocity can be shown from vacuum trajectory relationships to be

$$y_p = y_i \frac{\bar{V}_i^2 \cos^2\gamma_i}{1 + \sqrt{1 - \bar{V}_i^2(2 - \bar{V}_i^2)\cos^2\gamma_i}} - r_o\left[1 - \frac{\bar{V}_i^2 \cos^2\gamma_i}{1 + \sqrt{1 - \bar{V}_i^2(2 - \bar{V}_i^2)\cos^2\gamma_i}}\right] \tag{15}$$

where $\bar{V}_i$, the dimensionless velocity ratio, is

$$\bar{V}_i = \frac{V_i}{\sqrt{\mu/r}} = \frac{\text{resultant velocity at } y_i}{\text{local circular velocity at } y_i} \tag{16}$$

For entry at escape velocity, $\bar{V}_i = \sqrt{2}$, equation (15) becomes

$$y_p = y_i \cos^2\gamma_i - r_o(1 - \cos^2\gamma_i) \tag{17}$$

Vacuum perigee altitude is presented as a function of initial flight-path angle in figure 1 for entry at escape velocity from an initial altitude of 400,000 feet (V_i and y_i for the majority of the analysis).

Corridor depth for the spacecraft of the present report with $(L/D)_{max} = 0.5$ is also shown in figure 1 as a function of initial flight-path angle. A corridor depth of zero was chosen so that it corresponded to $\gamma_i = -5.03^\circ$. This is defined as the overshoot boundary since the spacecraft entering at the highest negative lift-drag ratio (-0.5) skip out of the atmosphere for entries with angles of descent less than 5.03°. The corridor depth increases as the initial angle of descent is increased, that is, as the undershoot boundary is lowered.

Spacecraft Drag Polars

Modulation is accomplished for each of the five drag polars of the present investigation by varying the spacecraft drag coefficient and lift-drag ratio during entry. The drag coefficients and lift-drag ratios are calculated on the assumption that the spacecraft have variations of lift and drag similar to that for (1) a parabolic drag polar (ref. 4),

(2) a flat plate in Newtonian flow (refs. 1 and 3), (3) a blunted half-cone, (4) a variable C_L, constant C_D drag polar (ref. 2), and (5) a variable C_D, constant C_L drag polar (ref. 3). The aerodynamic coefficients for these drag polars are tabulated below. The present

Drag polar	C_D	C_L	L/D
Parabolic	$C_{D_{min}} + \frac{C_L^2}{4C_{D_{min}}(L/D)^2_{max}}$	$2\left(\frac{L}{D}\right)_{max}\sqrt{C_{D_{min}}C_D - C_{D_{min}}^2}$	$2\left(\frac{L}{D}\right)_{max}\sqrt{\left(\frac{C_{D_{min}}}{C_D}\right) - \left(\frac{C_{D_{min}}}{C_D}\right)^2}$
Newtonian	$C_{D_{min}} + (C_{D_{max}} - C_{D_{min}})\sin^3\alpha$	$(C_{D_{max}} - C_{D_{min}})\sin^2\alpha \cos\alpha$	$\frac{(C_{D_{max}} - C_{D_{min}})\sin^2\alpha \cos\alpha}{C_{D_{min}} + (C_{D_{max}} - C_{D_{min}})\sin^3\alpha}$
Blunted half-cone	Wind tunnel results modified so that C_D at $C_{L_{max}}$, $C_{L_{max}}$, and $(L/D)_{max}$ are identical to that of the parabolic and Newtonian polars.		
Variable lift, constant drag	$C_{D_{min}}$	$0 \le C_L \le C_{L_{max}}$	$\frac{C_L}{C_{D_{min}}}$
Variable drag, constant lift	$C_{D_{min}} \le C_D \le C_{D_{max}}$	$C_{L_{max}}$	$\frac{C_{L_{max}}}{C_D}$

investigation is made for a range of values of maximum lift-drag ratio from 0.5 to 10. The particular drag polars employed with a maximum lift-drag ratio of 0.5 are shown in figure 2.

General Applicability of Results

The results of the present analysis can be applied to spacecraft of arbitrary weight and size because, as is shown in reference 6, many of the trajectory parameters are independent of m/C_DA. In this category are deceleration, velocity, flight-path angle, and range. Trajectory parameters that depend on m/C_DA are altitude and convective and radiative heating. The relationships for altitude and convective heating can be shown to be

$$y_2 - y_1 = \frac{1}{\beta}\log_e\left[\frac{(m/C_{D_i}A)_1}{(m/C_{D_i}A)_2}\right] \tag{18}$$

and

$$\frac{q_{c_2}}{q_{c_1}} \sim \frac{\dot{q}_{c_2}}{\dot{q}_{c_1}} \sim \sqrt{\frac{(m/C_{D_i}AR)_2}{(m/C_{D_i}AR)_1}} \tag{19}$$

The subscript 1 refers to values used in the present report and the subscript 2 corresponds to other values of $m/C_{D_i}A$ or $m/C_{D_i}AR$. Equations (9) and (18) and reference 7 can be used to calculate radiative heating if the velocity-time and velocity-altitude relationships are given.

The present results for each spacecraft can be shown to apply to families of spacecraft with similar drag polars having the same $(L/D)_{max}$ but different values of $C_{D_{max}}$ and $C_{D_{min}}$. This is possible for each family provided $C_{D_{max}}/C_{D_{min}}$ remains constant and m/A is adjusted to give initial values of m/C_DA equal to those used in the present investigation. The values of m/A used in the present investigation were selected so that, generally, each group of spacecraft with the same $(L/D)_{max}$ had the same m/C_DA at $(L/D)_{max}$. Thus, for entry with the same $(L/D)_{max}$, identical unmodulated undershoot trajectories are obtained for the same γ_i, V_i, and y_i. The values of m/A for the spacecraft with the drag polars shown in figure 2 are tabulated below.

Drag polar of figure 2*	m/A
Parabolic	1.98
Newtonian	3.00
Blunted half-cone	2.98
Variable lift, constant drag	3.61
Variable drag, constant lift	3.61

*$(L/D)_{max}$ = 0.5, m/C_DA at $(L/D)_{max}$ = 3.77

RESULTS AND DISCUSSION

To determine the effects of type of drag polar, initial velocity, initial flight-path angle, initial m/C_DA, and maximum lift-drag ratio on the reduction in maximum deceleration obtainable by modulation, unmodulated and modulated trajectories have been computed. Unmodulated entries are defined in this report as those during which the lift-drag ratios are held constant until the flight path is essentially horizontal ($\gamma \approx 0^\circ$, near maximum deceleration). To prevent skipping out of the atmosphere for the unmodulated undershoot entries with $L/D = (L/D)_{max}$, step changes to $L/D = -(L/D)_{max}$ and then back to $L/D = (L/D)_{max}$ were programmed to occur at points along the flight path so that decelerations greater than the first peak decelerations were avoided. To prevent excessive decelerations for the unmodulated overshoot entries with negative L/D, step changes to other values of L/D were made. For example, as described in reference 1 for the spacecraft with the Newtonian type drag polar ($(L/D)_{i_{ov}} = -(L/D)_{max} = -0.5$), a step change to $L/D = 0$ was made at $\gamma \approx 0^\circ$. All unmodulated overshoot entries were initiated with values of negative L/D which provided the highest overshoot vacuum perigee

altitude[1] and all unmodulated undershoot entries were initiated with $(L/D)_{max}$ to provide the lowest maximum deceleration. All modulated entries (undershoot entries only) were initiated with an L/D corresponding to that for $C_{L_{max}}$. For the variable C_L, constant C_D drag polar, this initial L/D is also $(L/D)_{max}$. (All results for the unmodulated and modulated entries at escape velocity with the Newtonian type drag polar with $(L/D)_{max} = 0.5$ have been reproduced from ref. 1.)

Maximum Deceleration

The effect of drag polar on the reduction in maximum deceleration obtainable by modulation is shown in figure 3 for entries at escape velocity for spacecraft with $(L/D)_{max} = 0.5$. The results are shown as the ratio of the minimum value of G_{max} for a modulated entry to G_{max} for an unmodulated entry ($(L/D)_i = (L/D)_{max}$) at the same initial flight-path angle. The results are for initial flight-path angles from about -5.7° to about -9.2°. The crosshatched areas represent variations in the G_{max} ratio for this range of γ_i.

A qualitative indication of the reduction in maximum deceleration obtainable by modulation can be obtained from an examination of the equations used to calculate the deceleration (see eqs. (13) and (14)). For a given spacecraft entering a planetary atmosphere at a given initial velocity, flight-path angle, m/C_DA, and L/D, it can be seen from these equations that for an unmodulated entry the deceleration varies directly as the dynamic pressure ($(1/2)\rho V^2$). As the spacecraft descends into the atmosphere, the dynamic pressure, and, hence, the deceleration, increases to a maximum value and then decreases. A typical deceleration time history for an unmodulated entry is shown by the solid curve in sketch (b). To maintain the maximum deceleration to a value lower than the peak value of the unmodulated entry (see the dashed curve in sketch (b)), the aerodynamic resultant-force coefficient C_R is continuously decreased to compensate for the increase in dynamic pressure (see eq. (13)). It was found in reference 4 that, for a given spacecraft entering at a given initial velocity and flight-path angle, the lowest possible maximum deceleration

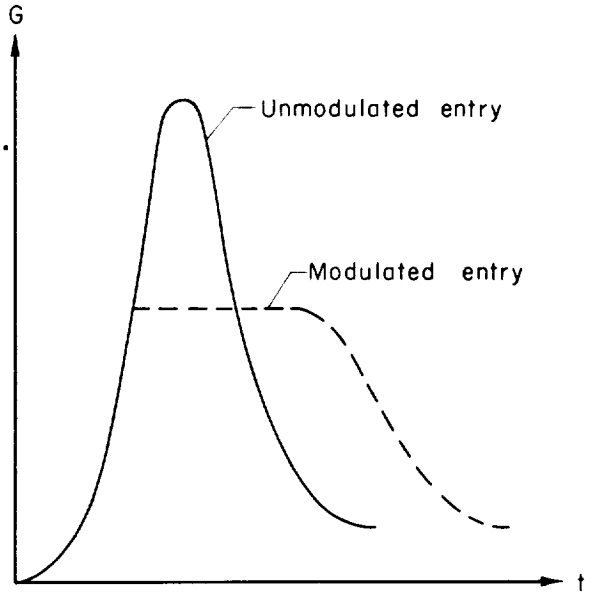

Sketch (b)

[1]As shown in reference 3, when the interdependence of L/D and C_D is considered, the highest overshoot vacuum perigee altitude is not necessarily obtained with $(L/D)_{i_{OV}} = -(L/D)_{max}$, and, as indicated in reference 5, should occur for entry at $-C_{L_{max}}$.

can be obtained if entry is initiated at the value of C_R for $C_{L_{max}}$ and C_R is continuously decreased to the value at $C_{D_{min}}$. This result suggests the ratio C_R at $C_{D_{min}}$ to C_R at $C_{L_{max}}$ as a parameter with which to correlate the maximum reduction in peak deceleration.

The ratio of minimum G_{max} for modulated entries to G_{max} for unmodulated entries is shown in figure 4 as a function of the ratio of C_R at $C_{D_{min}}$ to C_R at $C_{L_{max}}$ for a wide range of values of initial velocity, initial flight-path angle, initial m/C_DA, and maximum lift-drag ratio. The results are for all types of drag polars previously described, except the variable C_L, constant C_D drag polar.[2] For a given spacecraft (m/A and drag polar) and given initial velocity, the reductions in maximum deceleration shown represent the averages of the values obtained for a range of initial flight-path angles. In all cases, the actual fractional reduction in maximum deceleration agrees with the mean values shown in figure 4 to within ±1.5 percent (see, e.g., fig. 3). These results demonstrate for all drag polars investigated, except the variable C_L, constant C_D drag polar, that relative to the maximum deceleration of an unmodulated entry at $(L/D)_{max}$, the greatest reduction in maximum deceleration obtainable by modulation depends upon the ratio of C_R at $C_{D_{min}}$ to C_R at $C_{L_{max}}$; that is, the reduction in maximum deceleration is independent of initial velocity, initial flight-path angle, initial m/C_DA, maximum lift-drag ratio, and the shape of the drag polar. The fact that the fractional reduction in maximum deceleration is independent of initial velocity and initial flight-path angle was expected in view of similar results for the Newtonian type drag polar found in reference 1 for $(L/D)_{max} = 0.5$ and in reference 4 for any value of $(L/D)_{max}$.

For spacecraft with variable C_L, constant C_D drag polars, which operate from maximum lift-drag ratio to zero lift-drag ratio, the present results indicated that, relative to the maximum deceleration of an unmodulated entry at $(L/D)_{max}$, the greatest reduction in maximum deceleration obtainable by modulation depends upon the maximum lift-drag ratio. This relationship has been noted previously in reference 2. In fact, the reductions in maximum deceleration determined in the present investigation for variable C_L, constant C_D drag polars and those of reference 2 indicate that for values of $(L/D)_{max}$ as high as 3, the reduction in maximum deceleration obtainable is essentially proportional to $[1 + (L/D)^2_{max}]^{-1/2}$.

Corridor Depth

For spacecraft with the five drag polars with $(L/D)_{max} = 0.5$, figure 5 shows the corridor depth and corresponding initial flight-path angles for unmodulated and modulated entries at escape velocity as a

[2]For this drag polar, the lift-drag ratio initially decreases from $(L/D)_{max}$ rather than increasing toward $(L/D)_{max}$ as C_R decreases during modulation.

function of maximum deceleration. For a given maximum deceleration limit it can be seen that the use of modulation permits steeper entries, and thus, increased corridor depths. For example, consider an 8g-limited corridor. Without modulation a corridor depth of 27 international nautical miles can be obtained. For a spacecraft with the variable C_L, constant C_D drag polar, the use of modulation provides a corridor depth of about 29 international nautical miles. For a spacecraft with the parabolic drag polar, a corridor depth of 53 international nautical miles can be obtained if modulation is used.

The maximum increase in corridor depth obtainable by modulation can be correlated as shown in figure 6. As indicated

$$\frac{\left(y_{p_{ov_{unmod}}} - y_{p_{un_{mod}}}\right)_{max}}{y_{p_{ov_{unmod}}} - y_{p_{un_{unmod}}}} = 0.9388 - 1.5804 \log_{10} \frac{C_R \text{ at } C_{D_{min}}}{C_R \text{ at } C_{L_{max}}} \qquad (20)$$

Thus, the present data demonstrate that for all drag polars investigated, except the variable C_L, constant C_D drag polar, the maximum increase in corridor depth obtainable by modulation is essentially independent of initial velocity, initial m/C_DA, maximum lift-drag ratio, maximum deceleration, and shape of the drag polar.

Stagnation-Point Heating and Range

The results for stagnation-point heating (figs. 7 to 10) and range (fig. 11) are presented for the spacecraft with maximum lift-drag ratios of 0.5. All results are for entry at escape velocity from an altitude of 400,000 feet and are presented as functions of corridor depth and initial flight-path angle. To obtain the total heat and range for the unmodulated entries, the spacecraft were maneuvered as described earlier. The total heating and range for the modulated entries are shown only for those entries for which the trajectories remain within the atmosphere without requiring any additional maneuvering beyond that required to reduce G_{max}.

Since no specific spacecraft have been considered, the heating results are presented as heating parameters which contain $R^{1/2}$ and R^{-1} for convective and radiative heating, respectively. For different drag polars the shape of the spacecraft and, hence, R, is necessarily different. For a given drag polar, the value of R is not required to evaluate the effects of modulation on heating or the heating trends with corridor depth and initial flight-path angle. However, to evaluate the effects of drag polars, even for polars with the same $(L/D)_{max}$, a knowledge of R is required.

Maximum convective heating rate.- The maximum laminar convective heating-rate parameters for the unmodulated and modulated entries are shown in figure 7. The heating rates generally increased with increasing corridor depth and initial flight-path angle. For a given corridor depth, the heating rates for all entries are seen to depend primarily upon the radius of curvature of the spacecraft surface at the stagnation point.

Maximum radiative heating rate.- The maximum radiative heating-rate parameters for the unmodulated and modulated entries are presented in figure 8. The radiative heating rates increased with increasing corridor depth and flight-path angle. For a given corridor depth greater than about 20 international nautical miles, the peak radiative heating rates for the modulated entries were considerably less than the rates for the unmodulated entries, except for the variable C_L, constant C_D drag polar. For both unmodulated and modulated entries with this drag polar (same $(L/D)_i$ and the same $(m/C_DA)_i$), the peak radiative heating rates occurred prior to modulation.

Total convective heating.- The effect of modulation on the total convective heat absorbed per unit area at the stagnation point is indicated in figure 9. It is interesting to note that for a maximum deceleration of 10g, the parameters for total heat absorbed were approximately the same for all drag polars except the variable C_D, constant C_L drag polar (see tick marks in fig. 9). For the variable C_D, constant C_L drag polar, the trajectory for G_{max} = 10 skips out of the atmosphere and $\sqrt{R}\, q_c \approx 90 \times 10^3$ Btu $ft^{-3/2}$.

Total radiative heating.- It can be seen from figure 10 that the total radiative heat absorbed per unit area at the stagnation point was relatively insensitive to modulation, to drag polar, or to initial flight-path angle and depends primarily upon the radius of curvature of the spacecraft surface at the stagnation point.

Range.- It is evident from figure 11 that the range increased very rapidly for both the unmodulated and modulated entries as the corridor depth or initial flight-path angle was decreased to such values that the spacecraft were about to skip out of the atmosphere. It can be seen that greater ranges were obtained by the spacecraft with the variable C_D, constant C_L drag polar; however, these ranges were accompanied by decelerations in excess of 10g. The increased ranges occurred because at the end of the modulation period the spacecraft with the variable C_D, constant C_L drag polar was at maximum lift-drag ratio (L/D = 0.5); whereas, for all other drag polars, the spacecraft were at or near zero lift.

CONCLUDING REMARKS

Trajectories for unmodulated and modulated entries into the earth's atmosphere for a wide range of initial velocities and initial flight-path angles have been computed for lifting spacecraft with five basic types of drag polars. The parts of the drag polars of the spacecraft used during modulation were from maximum lift coefficient to minimum drag coefficient. The results indicate for all drag polars investigated, except a variable C_L, constant C_D drag polar, that relative to the maximum deceleration of an unmodulated entry at maximum lift-drag ratio, the greatest reduction in maximum deceleration obtainable by modulation depends only upon the ratio of the value of the aerodynamic resultant-force coefficient at minimum drag coefficient to the value at maximum lift coefficient. Thus, the reduction in maximum deceleration is independent of initial velocity, initial flight-path angle, initial m/C_DA, maximum lift-drag ratio, and the shape of the drag polar. For spacecraft with a variable C_L, constant C_D drag polar, the reduction in maximum deceleration was found to depend upon the quantity $[1 + (L/D)^2_{max}]^{-1/2}$. Also, relative to the depth of a given deceleration-limited corridor, the greatest increase in corridor depth obtainable by modulation (excepting the variable C_L, constant C_D drag polar) depends upon the ratio of C_R at $C_{D_{min}}$ to C_R at $C_{L_{max}}$. The fractional increase in corridor depth can be expressed as an empirically determined analytical function of this ratio.

Ames Research Center
National Aeronautics and Space Administration
Moffett Field, Calif., June 1, 1962.

REFERENCES

1. Katzen, Elliott D., and Levy, Lionel L., Jr.: Atmosphere Entries With Vehicle Lift-Drag Ratio Modulated to Limit Deceleration and Rate of Deceleration - Vehicles With Maximum Lift-Drag Ratio of 0.5. NASA TN D-1145, 1961.

2. Lees, Lester, Hartwig, Frederick W., and Cohen, Clarence B.: The Use of Aerodynamic Lift During Entry Into the Earth's Atmosphere. Space Tech. Labs. Rep. GM-TR-0165-00519, Nov. 1958. (Also GALCIT Pub. 462, and Amer. Rocket Soc. Jour., vol. 29, no. 9, Sept. 1959, pp. 633-641.)

3. Chapman, Dean R.: An Analysis of the Corridor and Guidance Requirements for Supercircular Entry Into Planetary Atmospheres. NASA TR R-55, 1960.

4. Grant, Frederick C.: Modulated Entry. NASA TN D-452, 1960.

5. Luidens, Roger W.: Approximate Analysis of Atmospheric Entry Corridors and Angles. NASA TN D-590, 1961.

6. Chapman, Dean R.: An Approximate Analytical Method for Studying Entry Into Planetary Atmospheres. NASA TR R-11, 1959.

7. Yoshikawa, Kenneth K., and Wick, Bradford H.: Radiative Heat Transfer During Atmosphere Entry at Parabolic Velocity. NASA TN D-1074, 1961.

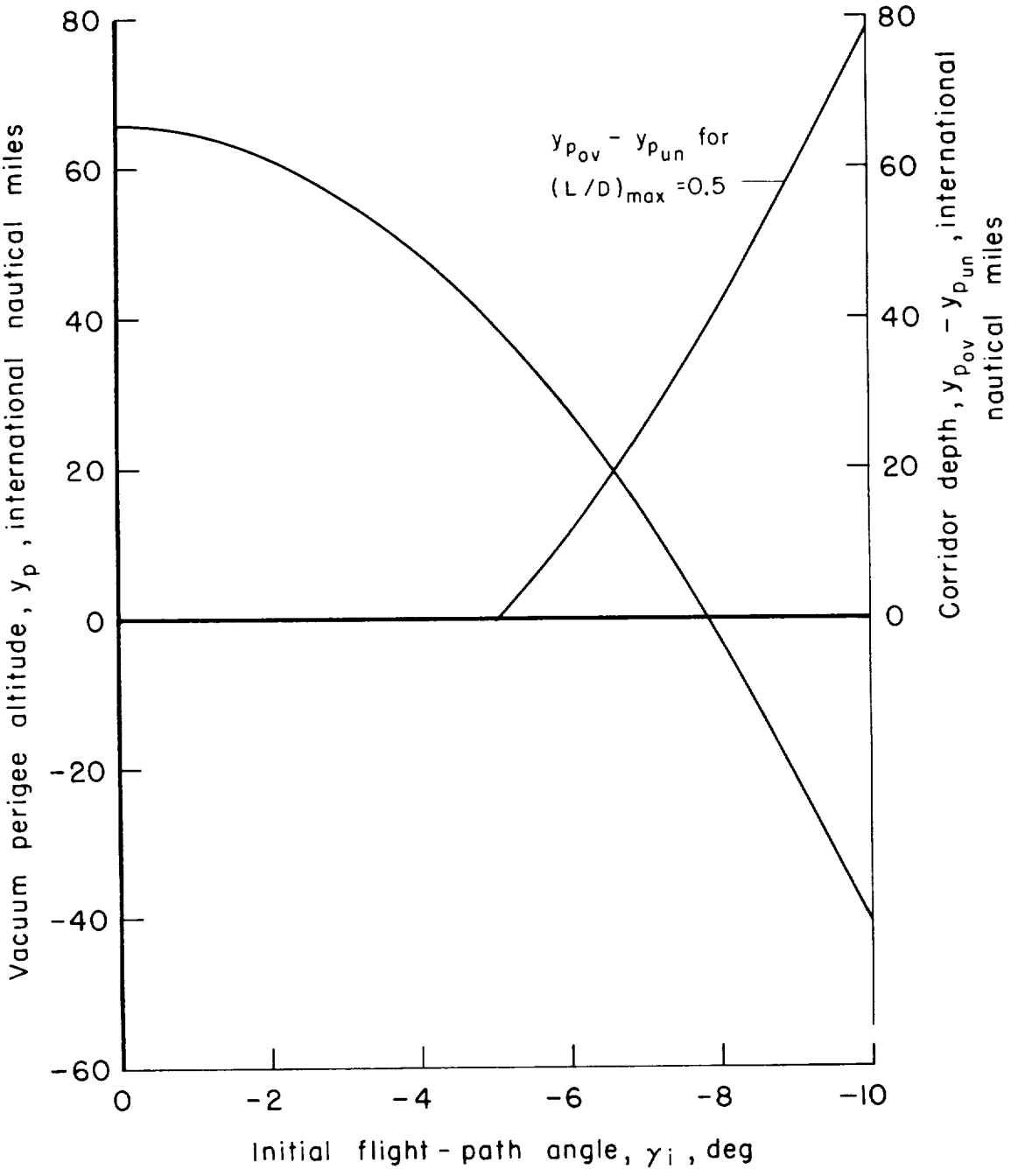

Figure 1.- Vacuum perigee altitude as a function of initial flight-path angle; y_i = 400,000 ft, V_i = 36,335 ft/sec.

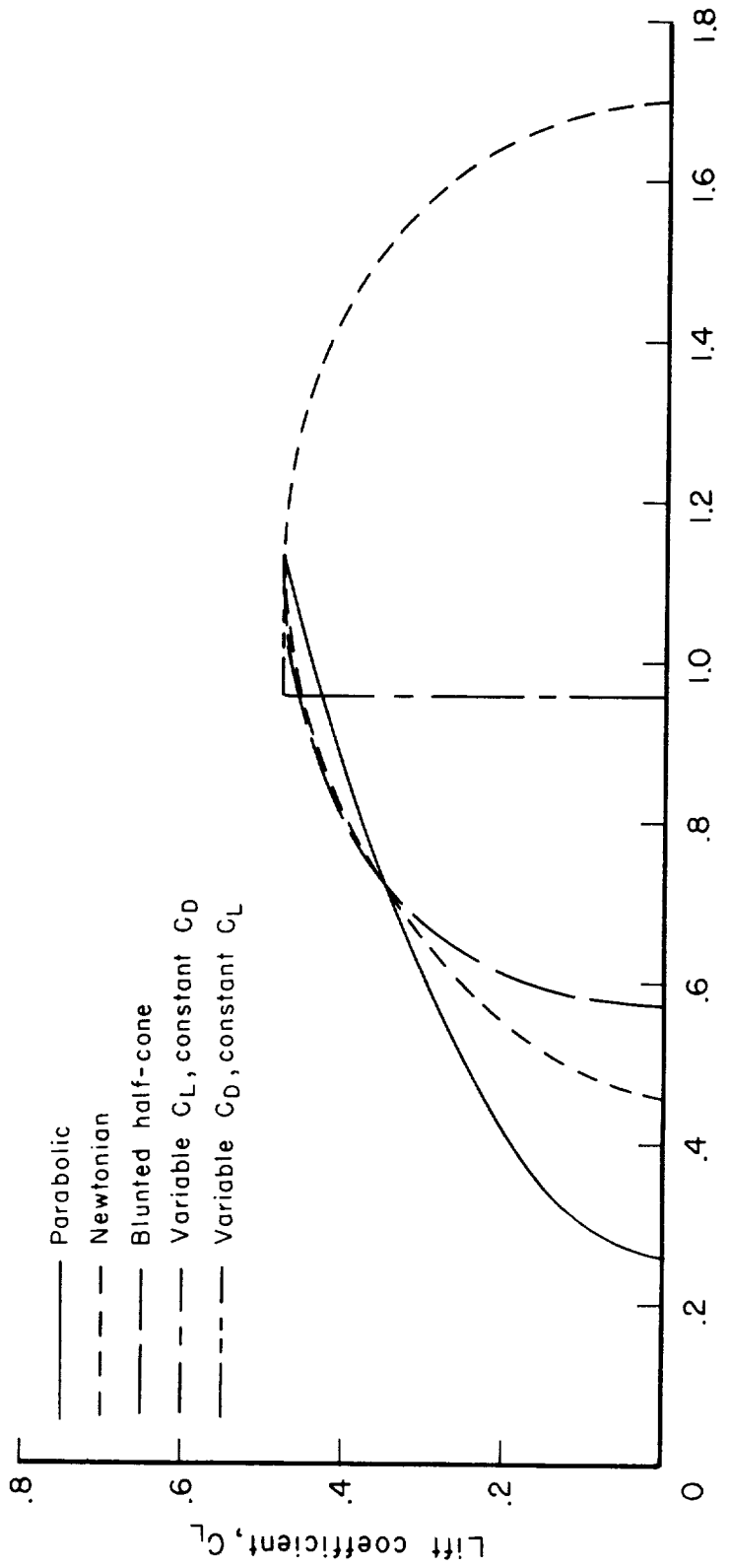

Figure 2.- Drag polars; $(L/D)_{max} = 0.5$.

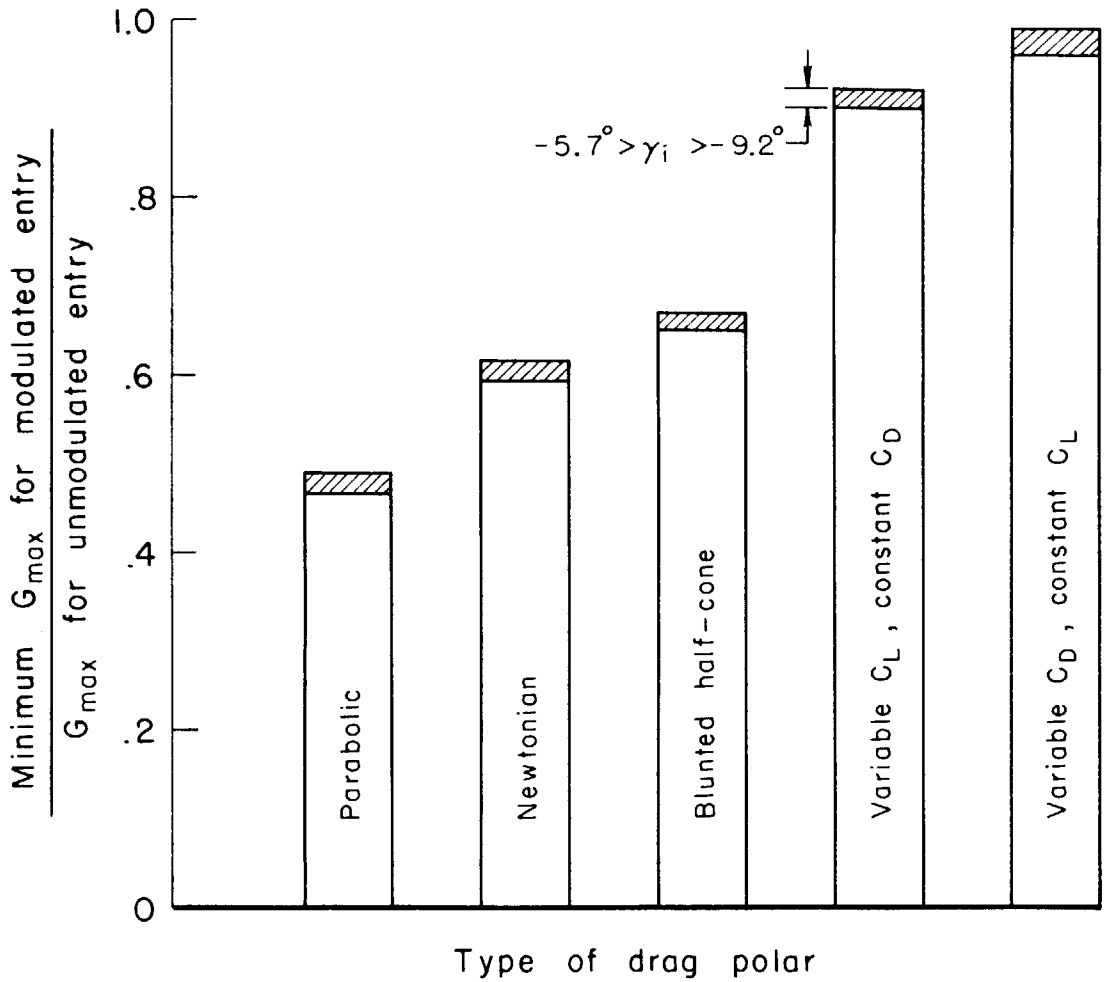

Figure 3.- Effect of drag polar on the maximum reduction in peak deceleration obtainable by modulation; $\overline{V}_i = \sqrt{2}$, y_i = 400,000 ft, $(L/D)_{i_{unmod}} = 0.5$, $(L/D)_{i_{mod}}$ = L/D at $C_{L_{max}}$, m/C_DA at $(L/D)_{max}$ = 3.7707 slugs/ft^2.

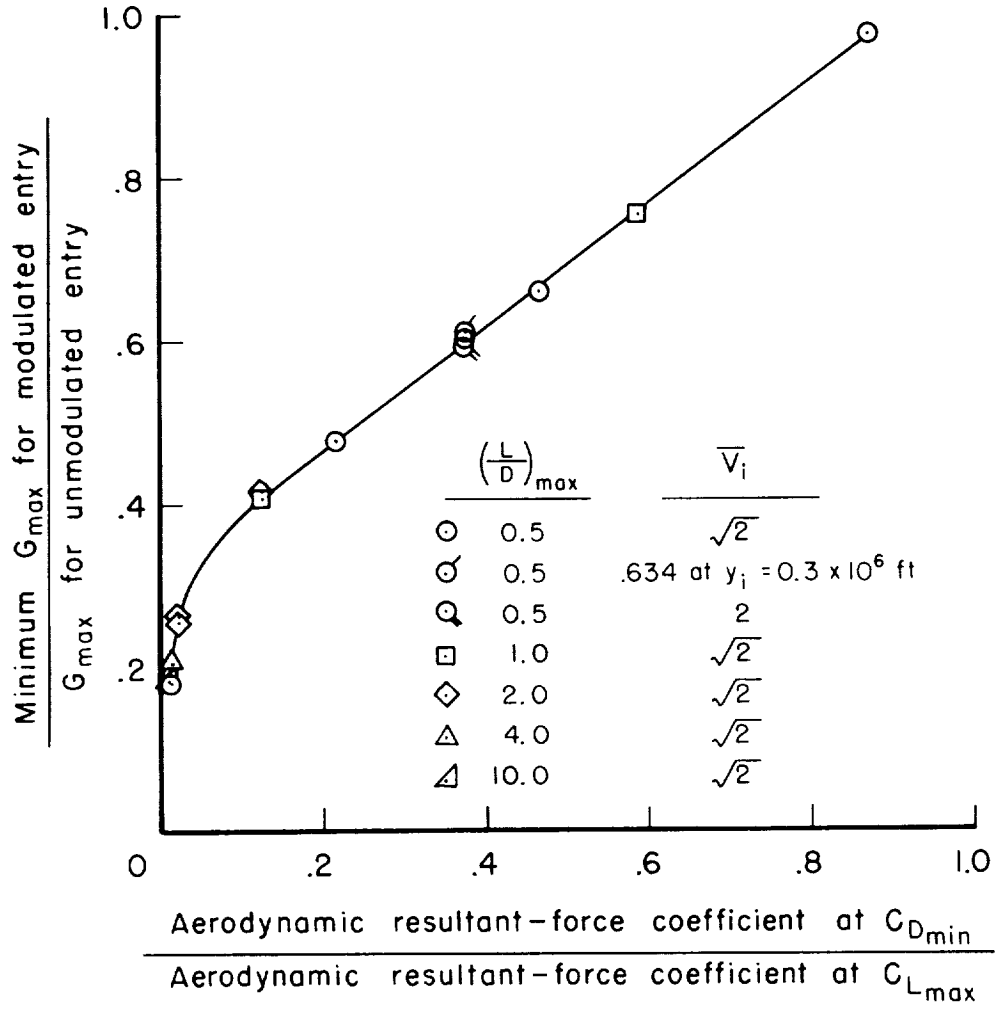

Figure 4.- Correlation of the maximum reduction in peak deceleration with the aerodynamic resultant-force coefficient; y_i = 400,000 ft, $-5.7^\circ > \gamma_i > -9.2^\circ$, $(L/D)_{i_{unmod}} = (L/D)_{max}$, $(L/D)_{i_{mod}}$ = L/D at $C_{L_{max}}$, 2 slugs/ft^2 < m/C_DA at $(L/D)_{max}$ < 42 slugs/ft^2.

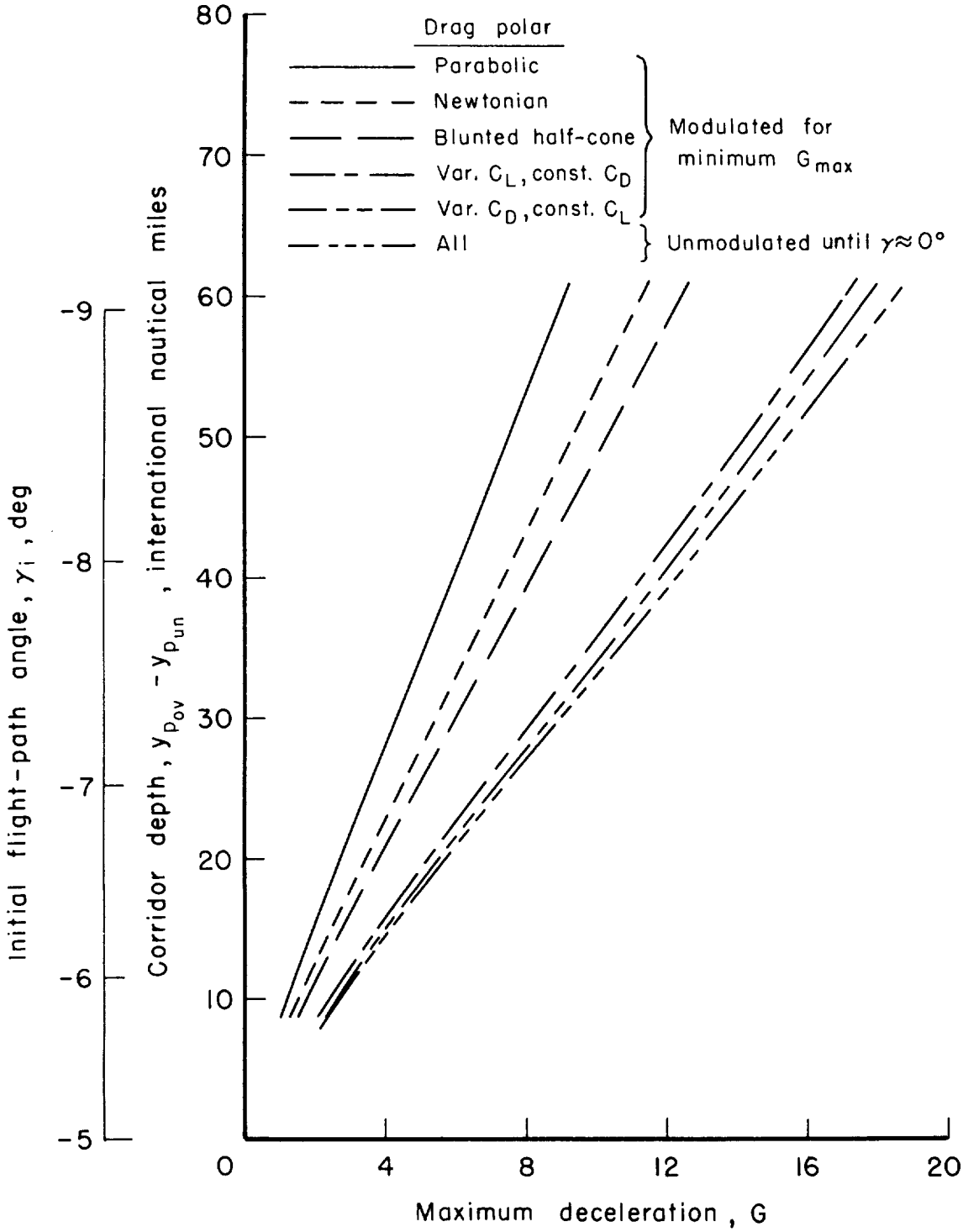

Figure 5.- Corridor depth and initial flight-path angle for unmodulated and modulated entries as a function of maximum deceleration; $\overline{V}_i = \sqrt{2}$, $y_i = 400{,}000$ ft, $(L/D)_{i_{unmod}} = 0.5$, $(L/D)_{i_{mod}} = L/D$ at $C_{L_{max}}$, m/C_DA at $(L/D)_{max} = 3.7707$ slugs/ft^2.

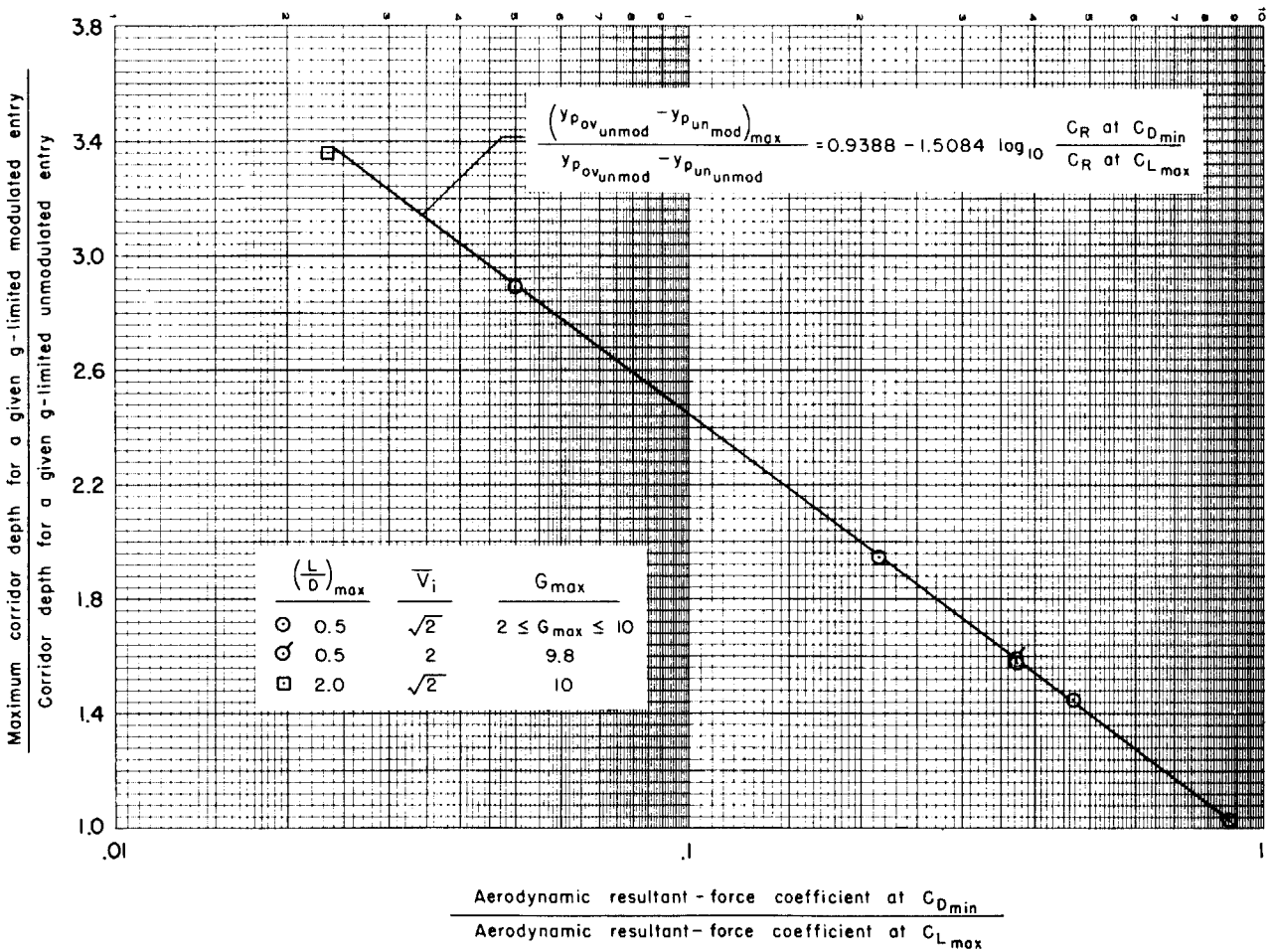

Figure 6.- Correlation of maximum increase in the depth of a given g-limited corridor with the aerodynamic resultant-force coefficient; y_i = 400,000 ft, $(L/D)_{i_{ov_{unmod}}}$ = -0.5, $(L/D)_{i_{un_{unmod}}} = (L/D)_{max}$, $(L/D)_{i_{un_{mod}}}$ = L/D at $C_{L_{max}}$, 2 slugs/ft^2 < m/C_DA at $(L/D)_{max}$ < 42 slugs/ft^2.

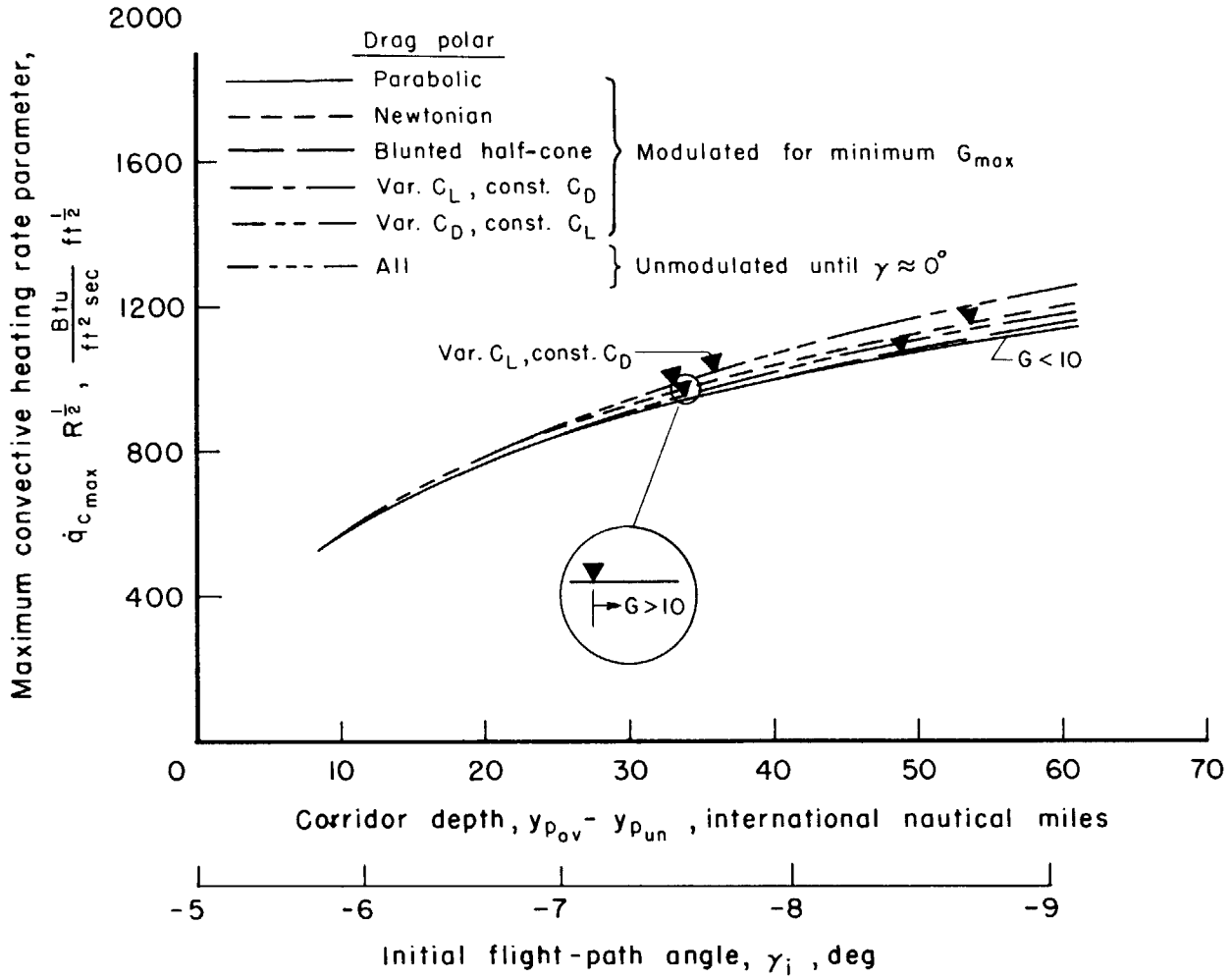

Figure 7.- Maximum laminar convective heating-rate parameters for unmodulated and modulated entries; $\overline{V}_i = \sqrt{2}$, y_i = 400,000 ft, $(L/D)_{i_{unmod}} = 0.5$, $(L/D)_{i_{mod}}$ = L/D at $C_{L_{max}}$, m/C_DA at $(L/D)_{max}$ = 3.7707 slugs/ft^2.

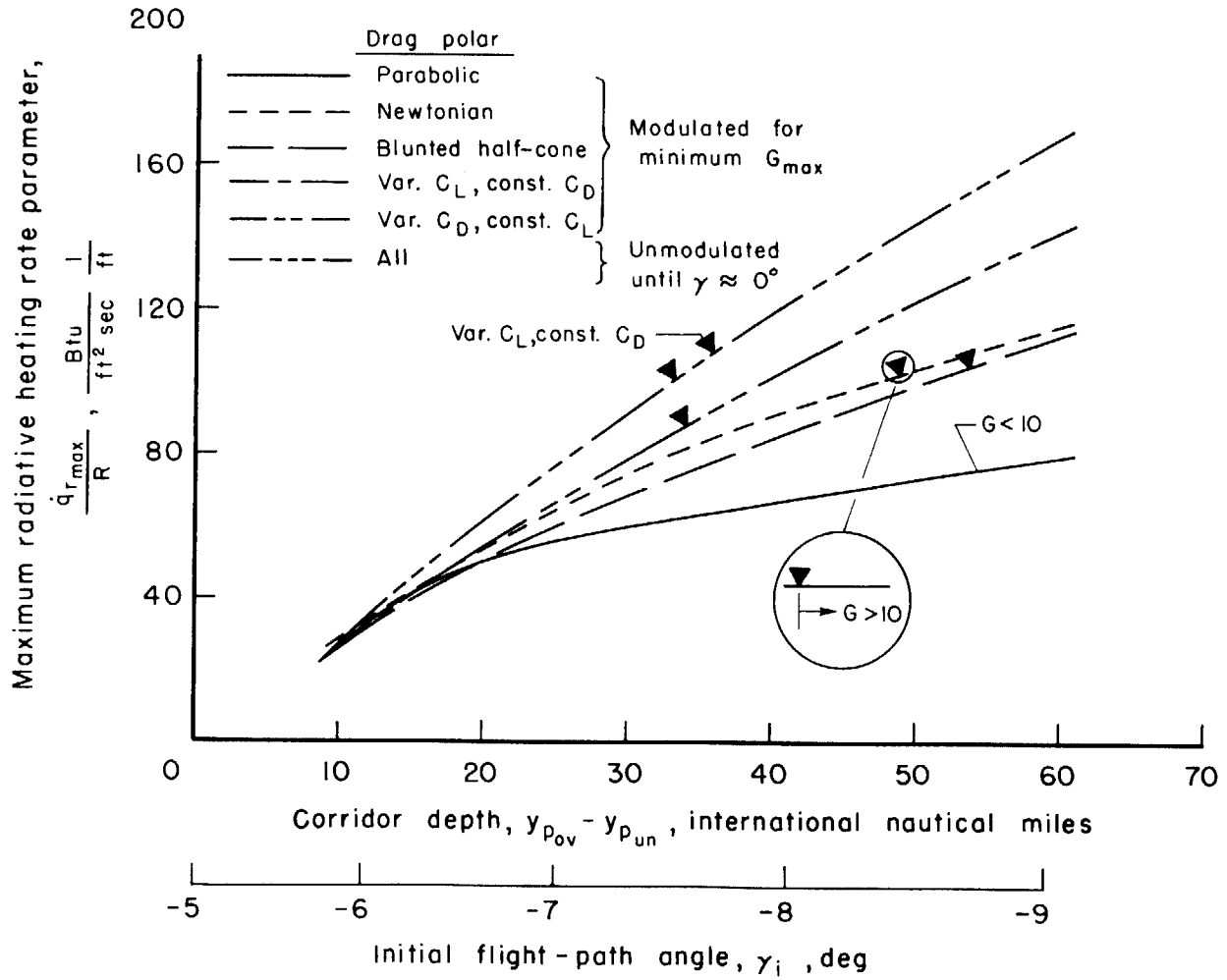

Figure 8.- Maximum equilibrium radiative heating-rate parameters for unmodulated and modulated entries; $\overline{V}_i = \sqrt{2}$, y_i = 400,000 ft, $(L/D)_{i_{unmod}} = 0.5$, $(L/D)_{i_{mod}}$ = L/D at $C_{L_{max}}$, m/C_DA at $(L/D)_{max}$ = 3.7707 slugs/ft^2.

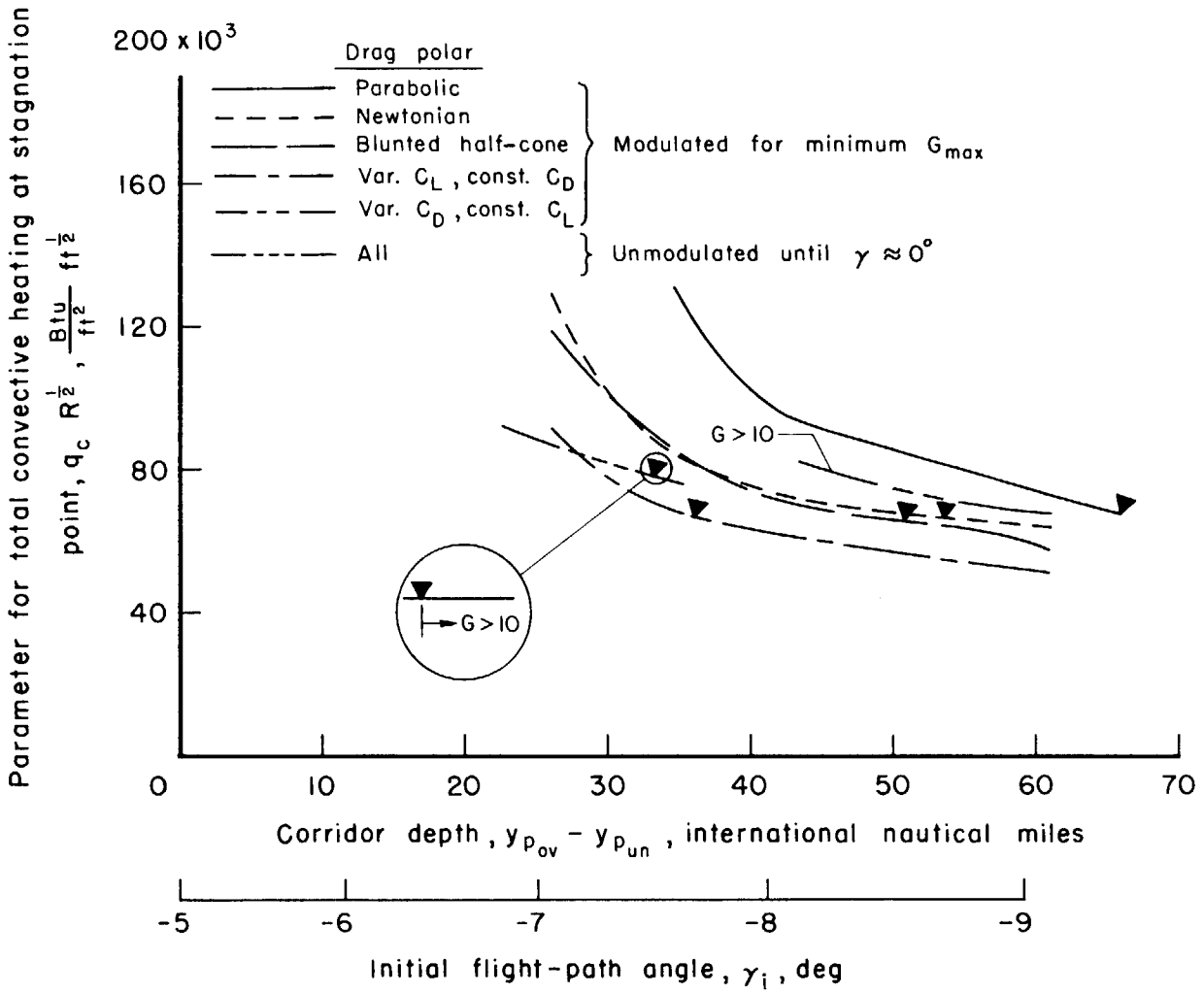

Figure 9.- Parameters for total laminar convective heating at stagnation point for unmodulated and modulated entries; $\overline{V}_i = \sqrt{2}$, y_i = 400,000 ft, $(L/D)_{i_{unmod}} = 0.5$, $(L/D)_{i_{mod}}$ = L/D at $C_{L_{max}}$, m/C_DA at $(L/D)_{max}$ = 3.7707 slugs/ft².

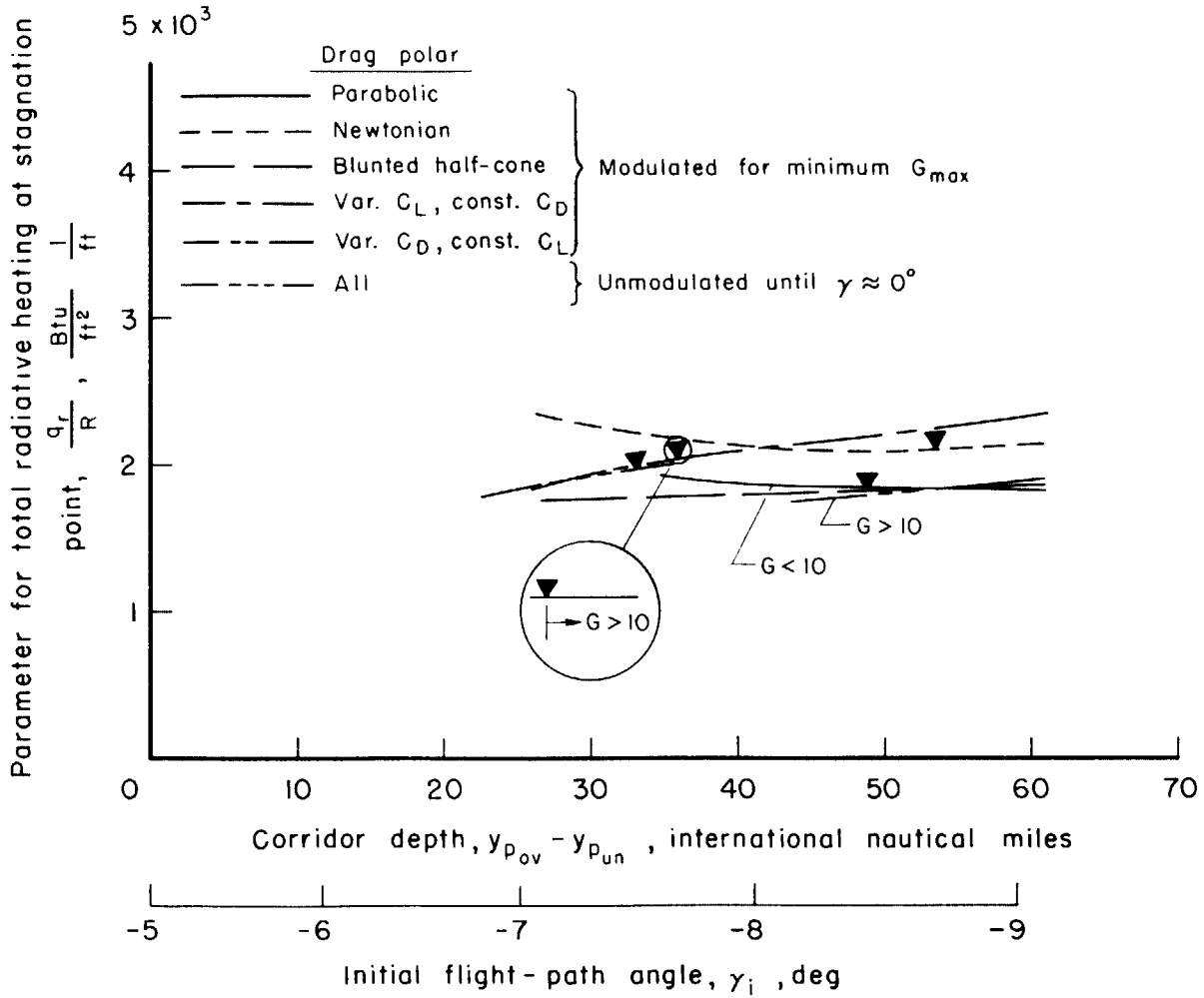

Figure 10.- Parameters for total equilibrium radiative heating at stagnation point for unmodulated and modulated entries; $\overline{V}_i = \sqrt{2}$, y_i = 400,000 ft, $(L/D)_{i_{unmod}} = 0.5$, $(L/D)_{i_{mod}}$ = L/D at $C_{L_{max}}$, m/C_DA at $(L/D)_{max}$ = 3.7707 slugs/ft^2.

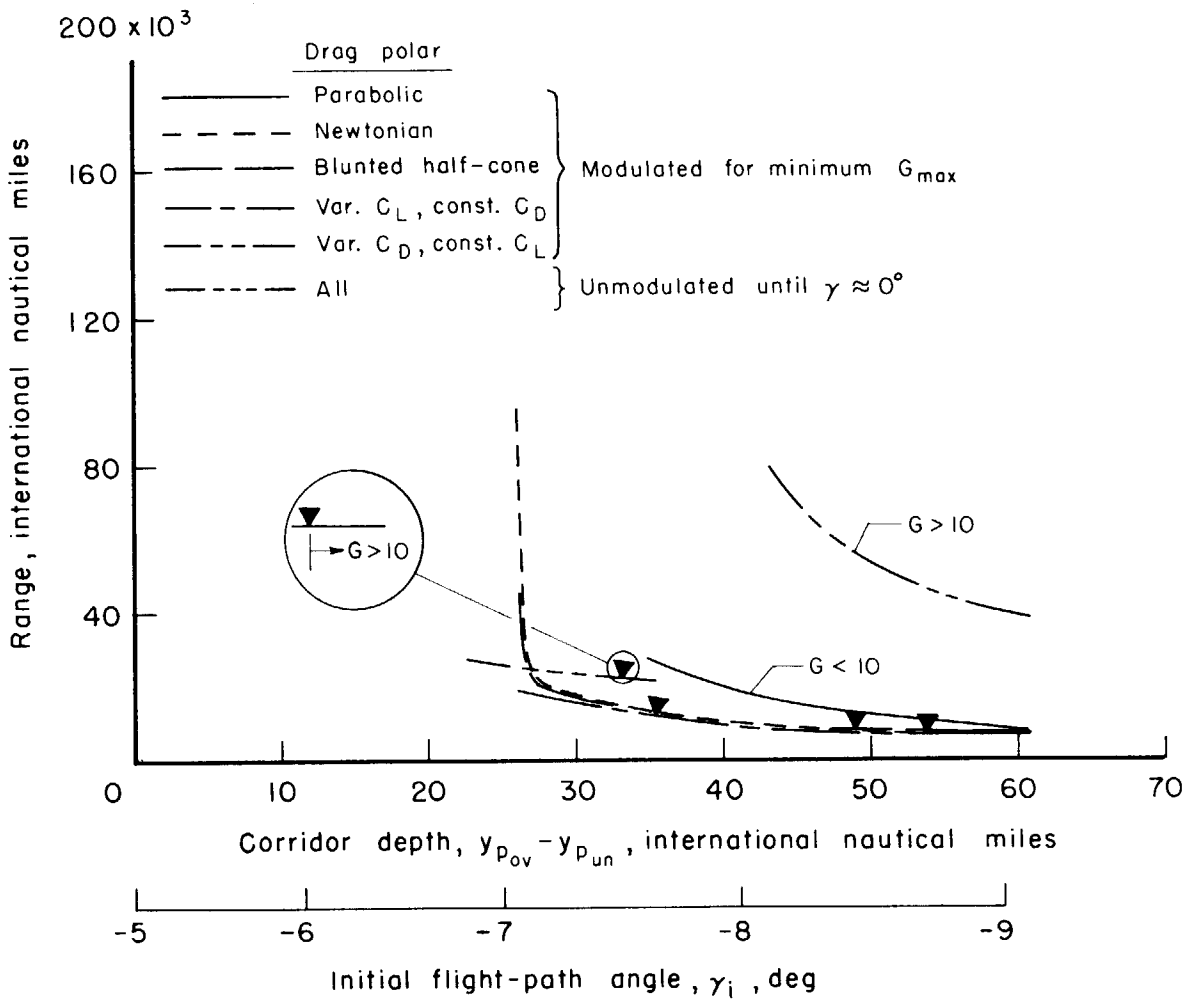

Figure 11.- Range for unmodulated and modulated entries; $\overline{V}_i = \sqrt{2}$, y_i = 400,000 ft, $(L/D)_{i_{unmod}} = 0.5$, $(L/D)_{i_{mod}}$ = L/D at $C_{L_{max}}$, m/C_DA at $(L/D)_{max}$ = 3.7707 slugs/ft^2.